Proc. IEEE Vehicular Technology Conference
Fall 2004 (VTC Fall 2004), Los Angeles (CA),
Sept. 2004, pp. 1443-1447.

Influence and Suppression of Phase Noise in Multi-Antenna OFDM

Tim C.W. Schenk*‡, Xiao-Jiao Tao*, Peter F.M. Smulders‡ and Erik R. Fledderus‡
*Agere Systems, PO Box 755, 3430 AT Nieuwegein, The Netherlands.
‡Eindhoven University of Technology, PO Box 513, 5600 MB Eindhoven, The Netherlands, T.C.W.Schenk@tue.nl.

***Abstract*— The influence of phase noise (PN) on the performance of a multiple-input multiple-output orthogonal frequency division multiplexing (MIMO-OFDM) based communication system is analyzed. As part of this analysis, an estimator for the common phase error (CPE) is derived, based on the maximum likelihood estimation (MLE), which was chosen for its asymptotic optimality. Since the computational complexity of the MLE procedure clearly rules out a cost effective solution, a reduced-complexity algorithm, based on least squares estimation (LSE) is designed which yields suboptimal performance. Simulation results reveal that the difference in bit-error-rate performance between systems applying the LSE or MLE of the CPE is very small. This implies that the LSE is well applicable for 802.11a based MIMO systems.**

I. Introduction

The application of multiple antennas at both transmitter (TX) and receiver (RX) side of wireless communication systems is proposed in many contributions over the last few years. This class of systems is often named multiple-input multiple-output (MIMO), referring to the multi-dimensional wireless channel. When applying this concept to wideband communication, the combination of MIMO architectures with the multicarrier technique orthogonal frequency division multiplexing (OFDM) is very promising. This combination, i.e., MIMO OFDM, enables the application of narrowband based MIMO techniques to every subcarrier separately. The potential of this physical layer design is clear from the numerous proposals in standardization, based on this concept, e.g., for Wireless Local-Area-Network (WLAN) in IEEE 802.11 and for Wireless Metropolitan-Area-Network (WMAN) in IEEE 802.16.

One of the major drawbacks of OFDM is the sensitivity of its performance to the radio impairment phase noise (PN) [1]–[3]. Several suppression schemes for PN in single-input single-output (SISO) OFDM systems have been proposed, among others, in [3]–[5] using either pilot data or decision feedback. The influence of PN on the performance of systems combining OFDM with multiple antenna techniques and suppression approaches are only treated in a few contributions [6], [7]. The case of space division multiple access (SDMA) combined with OFDM is treated in [6], where the different TX branches are not located in the same device, and thus experience independent PN processes. [6] proposes a suppression approach for the multiple PN processes based on least squares estimation (LSE). The analysis in [7] considers a MIMO system where the different TX and RX branches are co-located, and thus experience the same PN process. [7] shows that the inter-carrier interference (ICI) has spatial correlation. Taking this into account, a CPE estimation algorithm is proposed based on maximum likelihood (ML) theory.

This paper elaborates on the work in [7]. The influence of PN is derived analytically in Section II. The suppression algorithm proposed in [7] is extended in Section III to further improve its performance. This algorithm is shown to reduce to optimization of a concise determinant criterion. An implementation of the algorithm based on Gauss-Newton iterative techniques is given in Section III-B. To improve the applicability of the suppression, Section III-C proposes a sub-optimal algorithm with reduced computational complexity. From simulations with correlated fading channels the performance of the ML and the sub-optimal estimation approach are compared in Section IV. Furthermore, results from BER simulations show the performance for a 802.11a based multi-antenna OFDM system, implementing both suppression algorithms. Finally, conclusions are drawn in Section V.

II. Influence of PN on MIMO OFDM systems

Consider a MIMO OFDM system with N_t TX and N_r RX antennas, denoted here as a $N_t \times N_r$ system, applying N_c subcarriers. The branches at the TX (and similar for the RX branches) apply a common oscillator/frequency synthesizer (FS) and, thus, experience the same PN process. The system block diagram is depicted in Fig. 1.

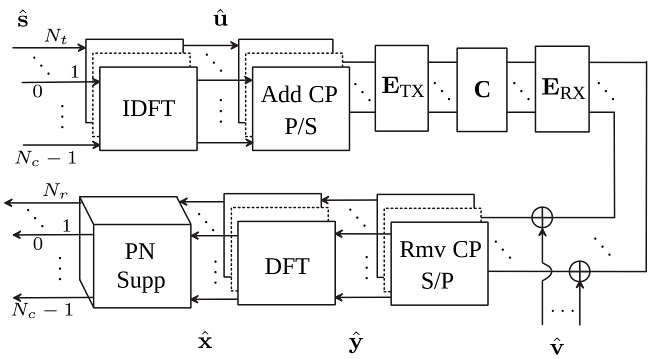

Fig. 1. MIMO OFDM system model with TX and RX PN impairments and PN suppression.

As detailed in [7], the received $N_cN_r \times 1$ frequency domain vector $\hat{\mathbf{x}}$, during the mth MIMO OFDM symbol period, is given by

$$\begin{aligned}\hat{\mathbf{x}}_m &= (\mathbf{F} \otimes \mathbf{I}_{N_r})\boldsymbol{\Upsilon}\mathbf{E}_{\mathrm{RX},m}(\mathbf{C}\mathbf{E}_{\mathrm{TX},m}\boldsymbol{\Theta}(\mathbf{F}^{-1} \otimes \mathbf{I}_{N_t})\hat{\mathbf{s}}_m + \hat{\mathbf{v}}_m) \\ &= (\mathbf{G}_{\mathrm{RX},m} \otimes \mathbf{I}_{N_r})\hat{\mathbf{H}}(\mathbf{G}_{\mathrm{TX},m} \otimes \mathbf{I}_{N_t})\hat{\mathbf{s}}_m + \hat{\mathbf{n}}_m \ , \qquad (1)\end{aligned}$$

where $\mathbf{F}$ is the $N_c \times N_c$ Fourier matrix, of which the (i,k)th element equals $\exp(-j2\pi\frac{ik}{N_c})$, $\mathbf{I}_N$ represents the $N \times N$ dimensional identity matrix, $\otimes$ denotes the Kronecker product and $\mathbf{\Theta}$ and $\mathbf{\Upsilon}$ represent the addition and removal of the cyclic prefix (CP), respectively. We assume that the CP length N_g is higher than the channel impulse response (CIR) length, preventing inter-symbol interference (ISI). The mth transmitted $N_cN_r \times 1$ MIMO OFDM symbol is given by $\hat{\mathbf{s}}_m = \left(\mathbf{s}_m^T(0), \mathbf{s}_m^T(1), \ldots, \mathbf{s}_m^T(N_c-1)\right)^T$, where $\mathbf{s}_m(n)$ denotes the $N_t \times 1$ frequency domain MIMO transmit vector for the nth subcarrier. $\mathbf{C}$ is the quasi-static multipath channel, with an average channel attenuation and delay of unity and zero, respectively. The frequency domain version channel is modelled by the $N_cN_r \times N_cN_t$ block diagonal matrix $\hat{\mathbf{H}}$. The nth $N_r \times N_t$ block diagonal element is $\mathbf{H}(n)$, the MIMO channel for the nth subcarrier. The $N_rN_c \times 1$ vector $\hat{\mathbf{n}}_m$ represents the frequency-domain noise, with i.i.d. zero-mean, complex Gaussian elements with a variance of σ_n^2 and $\hat{\mathbf{v}}_m$ denotes its time-domain equivalent.

The matrices $\mathbf{E}_{\text{TX}}$ and $\mathbf{E}_{\text{RX}}$ model the TX and RX PN impairment in this baseband (BB) signal model, respectively. $\mathbf{E}_{\text{TX},m}$ is given by $\text{diag}(e_{0,m}, e_{1,m}, \ldots, e_{N-1,m}) \otimes \mathbf{I}_{N_t}$, where $e_{i,m} = \exp(j\theta_{\text{TX}}(i+(m-1)N))$, $N = N_g + N_c$ is the length of the OFDM symbol in samples and i is the sample index within the symbol. Furthermore, θ_{TX} is a sampled random variable that represents the transmitter PN. $\mathbf{E}_{\text{RX}}$ is build up similar to $\mathbf{E}_{\text{TX}}$, but then based on θ_{RX}.

The second line in (1) is found by transforming the channel to the frequency domain and rewriting the influence of the PN to $\mathbf{G}_{\text{RX},m} = \mathbf{F}\mathbf{\Upsilon}\mathbf{E}_{\text{RX},m}\mathbf{\Theta}\mathbf{F}^{-1}$ and $\mathbf{G}_{\text{TX},m} = \mathbf{F}\mathbf{\Upsilon}\mathbf{E}_{\text{TX},m}\mathbf{\Theta}\mathbf{F}^{-1}$. The (k,l)th element of the $N_c \times N_c$ matrix $\mathbf{G}_{\text{TX},m}$, and similarly for $\mathbf{G}_{\text{RX},m}$, is given by

$$g_{k-l,m}^{\text{TX}} = \frac{1}{N_c} \sum_{i=0}^{N_c-1} e^{j\theta_{\text{TX}}((m-1)N+N_g+i)} e^{-j\frac{2\pi\{k-l\}i}{N_c}} \quad , \qquad (2)$$

Note that without PN, $\mathbf{G}_{\text{TX}}$ and $\mathbf{G}_{\text{RX}}$ reduce to identity matrices and all carriers are orthogonal. Estimates of the transmitted signal can be found by applying MIMO processing to the received signal $\hat{\mathbf{x}}_m$.

All elements on the diagonal of $\mathbf{G}_{\text{TX}}$ and $\mathbf{G}_{\text{RX}}$ are equal, i.e., g_0^{RX} and g_0^{TX}, respectively, and have unity amplitude. Since they are on the diagonal, they cause a rotation of the wanted signals. Since this rotation is equal for all carriers, it is often referred to as common phase error (CPE). The other elements in $\mathbf{G}_{\text{TX}}$ and $\mathbf{G}_{\text{RX}}$ cause interference among carriers, i.e., the ICI. We use this property to rewrite (1) to

$$\hat{\mathbf{x}}_m = \overbrace{g_{0,m}^{\text{RX}} g_{0,m}^{\text{TX}}}^{g_{0,m}} \hat{\mathbf{H}}\hat{\mathbf{s}}_m + \hat{\boldsymbol{\xi}}_m + \hat{\mathbf{n}}_m \quad , \qquad (3)$$

where

$$\hat{\boldsymbol{\xi}}_m = (\boldsymbol{\varphi}_{\text{RX},m} \otimes \mathbf{I}_{N_r})\hat{\mathbf{H}}(\boldsymbol{\varphi}_{\text{TX},m} \otimes \mathbf{I}_{N_t})\hat{\mathbf{s}} + g_{0,m}^{\text{RX}}\hat{\mathbf{H}}(\boldsymbol{\varphi}_{\text{TX},m} \otimes \mathbf{I}_{N_t})\hat{\mathbf{s}} + g_{0,m}^{\text{TX}}(\boldsymbol{\varphi}_{\text{RX},m} \otimes \mathbf{I}_{N_r})\hat{\mathbf{H}}\hat{\mathbf{s}}, \qquad (4)$$

$\boldsymbol{\varphi}_{\text{TX},m} = \mathbf{G}_{\text{TX},m} - g_{0,m}^{\text{TX}}\mathbf{I}_{N_tN_c}$ and $\boldsymbol{\varphi}_{\text{RX},m}$ has a similar structure as $\boldsymbol{\varphi}_{\text{TX},m}$. Thus, the first term in (3) is the desired signal times some common rotation $g_{0,m}$. The second term models the ICI, as worked out in (4). The last term in (3) models the additive white Gaussian noise (AWGN).

It is important to note that the ICI term (4) contains the complex channel matrix, which will have correlation over space, due to either the propagation channel or mutual coupling in the TX/RX chain including antennas and RF/analog front-end. Consequently, the ICI term will also exhibit correlation and is not independently and identically distributed (i.i.d.).

III. Estimation of common phase error

Phase noise primarily jeopardizes the performance of an OFDM system by the CPE, since it rotates the complex constellation points towards the decision boundaries, increasing the change of an erroneous detection. Due to its additive Gaussian character, the ICI is less destructive. Therefore, it is important to estimate and correct for the CPE, to suppress a large part of the influence of the PN.

Since the CPE changes on a symbol-by-symbol basis, it has to be estimated for every MIMO OFDM symbol. A convenient way to enable this estimation is insertion of pilot carriers in the transmitted symbols. We define the set of P pilot carrier number as $\mathcal{P} = \{p_1, p_2, \ldots, p_P\}$. From (3) it is clear the received signal, or observation vector, on pilot carriers p ($p \in \mathcal{P}$) during the reception of the mth MIMO OFDM is given by $\mathbf{x}_m(p) = g_{0,m}\mathbf{H}(p)\mathbf{s}_m(p) + \boldsymbol{\xi}_m(p) + \mathbf{n}_m(p)$. Since coherent detection is regarded, the channel matrix $\mathbf{H}(p)$ is assumed to be available by channel training and $\mathbf{s}_m(p)$ are pilots and thus known. This enables the estimation of $g_{0,m}$.

A. Maximum likelihood estimator

As noted in Section II, the ICI term exhibits spatial correlation, making suppression approaches proposed for SISO OFDM [3]–[5], which assume i.i.d. noise terms, not directly applicable to the MIMO case. To understand the best attainable performance, an exact maximum likelihood estimator (MLE) is chosen for its well-known asymptotic optimality.

Similarly to the derivation in [8], we assume the observation noise $\mathbf{z}_m(p) = \mathbf{x}_m(p) - g_{0,m}\mathbf{H}(p)\mathbf{s}_m(p) = \boldsymbol{\xi}_m(p) + \mathbf{n}_m(p)$ is multivariate complex normally distributed with the unknown $N_r \times N_r$ covariance $\mathbf{\Omega}$, i.e., $\mathbf{z}_m(p) \sim \mathcal{CN}(\mathbf{0}, \mathbf{\Omega})$ for $p \in \mathcal{P}$. Furthermore, it is assumed that the estimation errors on the different pilot carriers are uncorrelated, but that the estimation errors on the same pilot carriers on the different RX antennas are correlated.

As noted, $g_{0,m}$ is a function of the symbol index m and thus changes over time. Also the observation noise changes over time, but its covariance matrix stays constant, since the channel is quasi-static. We exploit this fact by simultaneously estimating the vector $\mathbf{g_0} = (g_{0,1}, g_{0,2}, \ldots, g_{0,M})$, where M is the number of symbol in the regarded packet. Clearly this approach improves the performance achieved by the algorithm proposed in [7], which separately estimates all CPE terms in $\mathbf{g_0}$ and, thus, does not exploit the fact that the covariance matrix is constant over time.

The joint probability density function, conditional on all unknown parameters, is given by

$$p(\mathbf{z}|\mathbf{g_0},\mathbf{\Omega}) = \frac{(\pi)^{-PMN_r}}{\det(\mathbf{\Omega})^{PM}} \exp\left(-\sum_{m=1}^{M}\sum_{p\in\mathcal{P}} \mathbf{z}_m^H(p)\mathbf{\Omega}^{-1}\mathbf{z}_m(p)\right) \quad (5)$$

When we now define the $P \times N_r$ matrix $\mathbf{Z}_m = [\mathbf{z}_m(p_1), \mathbf{z}_m(p_2), \ldots, \mathbf{z}_m(p_P)]^H$, the joint probability density function of (5) can be written as

$$p(\mathbf{Z}|\mathbf{g_0},\mathbf{\Omega}) = \frac{(\pi)^{-PMN_r}}{\det(\mathbf{\Omega})^{PM}} \exp\left(-\sum_{m=1}^{M} \mathrm{tr}(\mathbf{Z}_m\mathbf{\Omega}^{-1}\mathbf{Z}_m^H)\right) \ . \quad (6)$$

The MLE is then given by maximizing the log-likelihood (LL) function $\ln\left(p(\mathbf{Z}|\mathbf{g_0},\mathbf{\Omega})\right)$, which is given by

$$L(\mathbf{g_0},\mathbf{\Omega}) = C_1 + PM\ln(\det(\mathbf{\Omega}^{-1})) - \sum_{m=1}^{M} \mathrm{tr}\left(\mathbf{Z}_m\mathbf{\Omega}^{-1}\mathbf{Z}_m^H\right) \ , \quad (7)$$

where C_1 denotes a constant. Setting the partial derivative of the LL function with respect to $\mathbf{\Omega}$ to zero gives the conditional estimate $\bar{\mathbf{\Omega}} = \sum_{m=1}^{M}(\mathbf{Z}_m^H\mathbf{Z}_m)/\,(PM)$ [9]. When this is substituted in (7), the conditional LL function is given by

$$L(\mathbf{g_0},\bar{\mathbf{\Omega}}) = C_2 - PM\ln\left\{\det\left(\sum_{m=1}^{M}\mathbf{Z}_m^H\mathbf{Z}_m\right)\right\} \ , \quad (8)$$

where C_2 denotes a constant. Maximizing this log-likelihood function then equals minimizing

$$\mathbf{\Phi}(\mathbf{g_0}) \ = \det\left(\sum_{m=1}^{M}\sum_{p\in\mathcal{P}}\mathbf{z}_m(p)\mathbf{z}_m^H(p)\right) \ . \quad (9)$$

The elements of $\mathbf{g_0}$ represent phase rotations and have an amplitude of 1. Therefore, they are fully characterized by their phases $\boldsymbol{\vartheta} = (\vartheta_1, \vartheta_2, \ldots, \vartheta_M)$. The estimation of $\boldsymbol{\vartheta}$ is preferred, since $\boldsymbol{\vartheta}$ only contains real variables, and will thus be regarded in the remainder of the paper.

B. MLE optimization algorithm

The minimization of the determinant criterion (9), or cost function $\mathbf{\Phi}(\mathbf{g_0})$, can be implemented using several optimalization techniques. An iterative technique, based on the Gauss-Newton algorithm, which is well established for problems like (9) [8], is chosen here.

The algorithm can, for this linear case, be summarized as follows:

1) Set the iteration number k to 0 and select a feasible initial estimate for $\boldsymbol{\vartheta}^{(0)}$.
2) Stop if the convergence criterion is reached.
3) Calculate the gradient vector $\mathbf{d}^{(k)}$ and the Hessian matrix $\mathbf{G}^{(k)}$, i.e., the matrix of second derivatives.
4) Solving the search direction vector $\boldsymbol{\delta}^{(k)}$ from $\mathbf{G}^{(k)}\boldsymbol{\delta}^{(k)} = -\mathbf{d}^{(k)}$.
5) Set $\boldsymbol{\vartheta}^{(k+1)} = \boldsymbol{\vartheta}^{(k)} + \boldsymbol{\delta}^{(k)}$ and $k = k+1$. Return to Step 2.

Here $\boldsymbol{y}^{(k)}$ denotes the vector $\boldsymbol{y}$ during the kth iteration.

In Step 3 the gradient $\mathbf{d}$ and the Hessian $\mathbf{G}$ have to be calculated. The gradient $\mathbf{d} = \partial\mathbf{\Phi}(\boldsymbol{\vartheta})/\partial\boldsymbol{\vartheta}$, where $\mathbf{\Phi}(\boldsymbol{\vartheta})$ is easily found from by substituting $\mathbf{g_0}$ in (9) by $\cos(\boldsymbol{\vartheta}) + j\sin(\boldsymbol{\vartheta})$. The (q,r)th element of the Hessian is given by $G_{q,r} = \partial^2\mathbf{\Phi}(\boldsymbol{\vartheta})/\,(\partial\vartheta_q\partial\vartheta_r)$. The exact calculation of the gradient and Hessian is given in Appendix I.

An important part of the optimization algorithm is the convergence criterion used. Since the cost function was found to be quadratic from visual inspection, a relative simple convergence criterion was anticipated to suffice. Therefore, the relative increment of the parameters compared to the previous iteration was chosen as convergence measure, which is given by

$$\left|\frac{\boldsymbol{\vartheta}^{(k)} - \boldsymbol{\vartheta}^{(k-1)}}{\boldsymbol{\vartheta}^{(k)}}\right| \le \epsilon \quad (10)$$

where ϵ is the tolerance level. The choice of ϵ depends on the required accuracy.

C. Least squares estimator

The computational complexity of the MLE procedure clearly rules out a cost-effective solution. Therefore a sub-optimal algorithm is studied, where we diverge from the original constraints and assume the correlated ICI is not dominant in the estimation noise $\mathbf{z}_m(p)$, i.e., the covariance matrix $\mathbf{\Omega}$ in (5) can be approximated with a diagonal matrix. The determinant of $\mathbf{\Omega}$ then reduces to the product of its elements and maximizing the LL function equals maximizing the exponent term in (6). Then, under this widely used but more strict i.i.d white Gaussian distributed noise assumption, the MLE reduces to the least-square estimator (LSE) [7].

The well known solution of the LS problem is given by

$$\widetilde{g}_{0,m} = \mathbf{A}_{m,\mathcal{P}}^{\dagger}\mathbf{x}_{m,\mathcal{P}} = \left\{\mathbf{A}_{m,\mathcal{P}}^H\mathbf{A}_{m,\mathcal{P}}\right\}^{-1}\mathbf{A}_{m,\mathcal{P}}^H\mathbf{x}_{m,\mathcal{P}} \ , \quad (11)$$

where $\mathbf{A}_{m,\mathcal{P}} = \mathbf{H}_{m,\mathcal{P}}\mathbf{s}_{m,\mathcal{P}}$. The received signal vector on the collection of pilot carriers is given by the $PN_r \times 1$ vector $\mathbf{x}_{m,\mathcal{P}} = (\mathbf{x}_m^T(p_1), \mathbf{x}_m^T(p_2), \ldots, \mathbf{x}_m^T(p_P))^T$. The vector $\mathbf{s}_{m,\mathcal{P}}$ is built up similarly. The kth block diagonal element of the $PN_r \times PN_t$ block diagonal channel matrix $\mathbf{H}_{\mathcal{P}}$ is given by the $N_r \times N_t$ matrix $\mathbf{H}(p_k)$.

Recalling that the channel is quasi-static, hence if the pilot tones in the packet are equal for the consecutive OFDM symbols, it is sufficient to calculate the pseudo-inverse $\mathbf{A}_{m,\mathcal{P}}^{\dagger}$ only once per packet. Clearly, the complexity of this algorithm is much lower than that of the MLE optimization.

It is noted that the 1×1 version of this reduced-complexity algorithm is equal to the one proposed in [2]. Furthermore, [7] gives an analytical upper bound on the mean squared error of the LSE of the CPE as function of the frequency of the PN process. It is concluded that lower frequencies are best estimated, which can be explained by the low time resolution of the observations (once every N samples). Furthermore, the MSE decreases linearly with the number of RX antenna N_r and pilots P.

IV. SIMULATION RESULTS

Simulations were carried out to evaluate the performance of the estimators proposed in Section III. Furthermore, a goal was to test the performance of a MIMO OFDM system experiencing PN and applying the proposed suppression techniques. As a test case, a MIMO extension of the IEEE 802.11a WLAN standard [10] was studied. The applied parameters are: modulation = 64 QAM, bandwith = 20 MHz, number of subcarriers N_c = 64, number of pilot carriers P = 4, guard interval length N_g = 16, coding rate = 1.

In all simulations the PN is modelled in the RX using a Lorentzian power spectral density (PSD), defined by the total integrated PN power P_{pn} and corner frequency f_c.

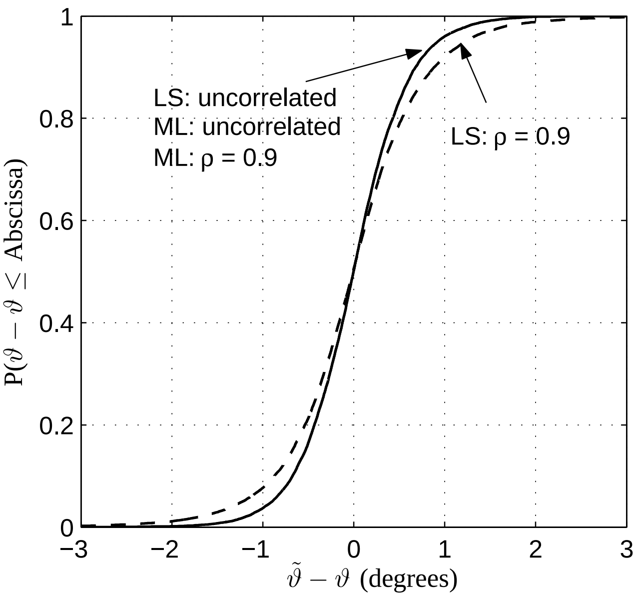

Fig. 2. ECDF of the error in estimation of ϑ for a 2×2 configuration, P_{pn} = −30 dBc and f_c = 200 kHz, 20 symbols per packet, $\rho = 0$ (uncorrelated case) and $\rho = 0.9$, independent Rayleigh fading.

Fig. 2 depicts the empirical cumulative distribution function (ECDF) of the error in the estimation of the phase of the CPE term, $\vartheta = \angle g_0$, for both the MLE and LSE. The PN parameters are $P_{\text{pn}} = -30$ dBc and $f_c = 200$ kHz. Twenty MIMO OFDM symbols are transmitted per packet. The results are shown for no spatial correlation ($\rho = 0$) and for a correlation between the two branches of 0.9 at both TX and RX, where the correlation model from [11] is used. The different subcarriers on one branch experience independent Rayleigh fading. No WGN receiver noise is added, to investigate the influence of the ICI.

It is clear from the results in Fig. 2 that the ML and LS estimator have the same performance in spatial uncorrelated channels. Furthermore, it is observed that the estimation is unbiased. When the spatial correlation is increased to 0.9, the MLE performance does not degrade, while the performance of the LSE does.

Fig. 3 shows the mean squared error (MSE) of the estimated angle ϑ (in degrees), as function of the signal-to-noise ratio

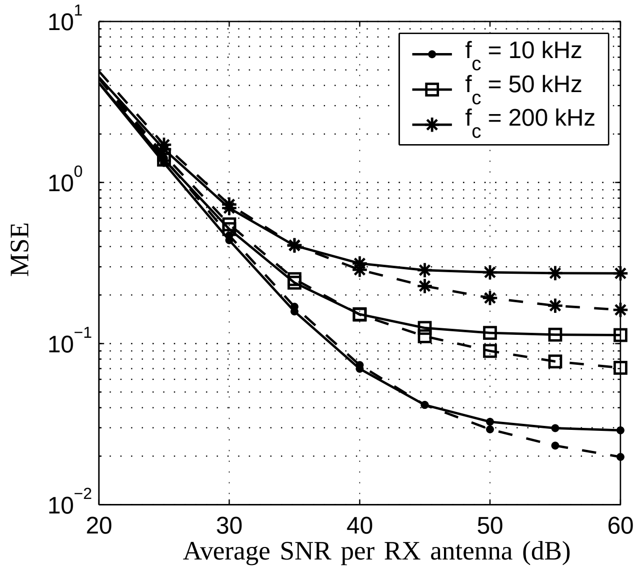

Fig. 3. MSE in estimation of ϑ (in degrees) for a 2×2 configuration for MLE (−−) and LSE (—), P_{pn} = −30 dBc, 5 OFDM symbols per packet, $\rho = 0.7$, flat Rayleigh fading.

(SNR). $P_{\text{pn}} = -30$ dBc and f_c is varied. A flat fading Rayleigh channel is applied, with correlation between the TX and RX elements of $\rho = 0.7$.

The figure shows that for low SNR values the performance of the LSE and MLE are similar, but that at high SNR values the LSE shows a higher error floor than the MLE. This is explained by the spatially correlated ICI which becomes dominant at high SNR values. As noted before, the performance of the LSE is worse in correlated ICI than that of the MLE.

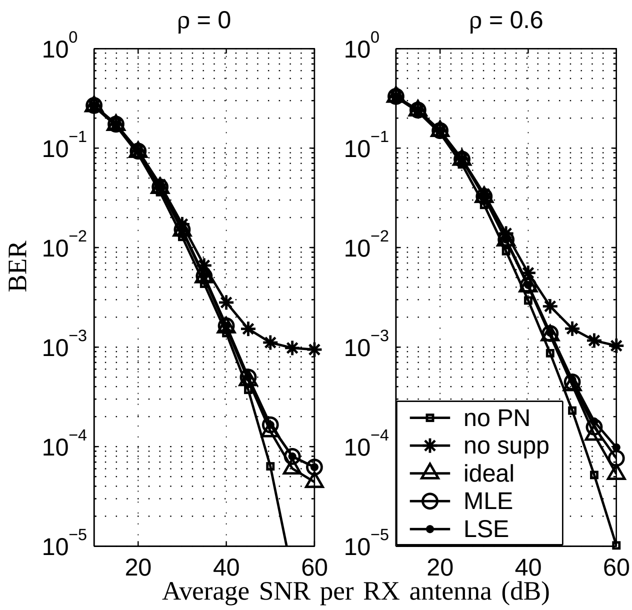

Fig. 4. BER for a 2×2 ZF receiver for no PN, no suppression and ideal, MLE and LSE based CPE correction. P_{pn} = −24 dBc and f_c = 100 kHz, 5 OFDM symbols per packet, $\rho = 0$ and 0.6, flat Rayleigh fading.

Another observation that can be made from Fig. 3, is that the performance of both estimators decreases with increasing

f_c. This is explained by the power of ϑ and the ICI term that decrease and increases, respectively, with increasing f_c.

The results from bit-error rate (BER) simulations with a zero-forcing RX, as depicted in Fig. 4, show that the CPE correction clearly improves the BER performance compared the case where no suppression is applied (*no supp* in Fig. 4). For both $\rho = 0$ and $\rho = 0.6$, the performance of the MLE and LSE based CPE correction is only a little worse than that of the ideal correction. For $\rho = 0$ the performance of the MLE and LSE based correction is similar, while for $\rho = 0.6$ the MLE is a little better, but only for very high SNR values.

V. Conclusions

The influence of phase noise (PN) in a multi-antenna OFDM system was studied. Similar as in conventional single antenna OFDM systems, studied in previous contributions, the PN causes a common phase rotation (or CPE) of the desired signals. Furthermore, an additive inter-carrier interference (ICI) term occurs. It is noted that since the channel is contained in the expression for the ICI, the ICI will, differently from the single antenna case, exhibit spatial correlation.

An estimator for the CPE, based on maximum likelihood (ML) theory, was derived. The estimator was shown to be equivalent to optimizing a concise determinant criterion. Implementation of the MLE using a Gauss-Newton based iterative solution was proposed. Since the computational complexity of the MLE procedure rules out a cost-effective solution, a suboptimal algorithm was studied, based on least-square estimation (LSE).

Simulations were performed for a system based on a MIMO extension of IEEE 802.11a. The results show that in case of uncorrelated MIMO channels the LSE and MLE have similar performance, as was anticipated from theory. In case of spatial correlation the MLE performs better. Regarding the mean squared error (MSE) of the CPE estimation as function of the SNR, the performance of the LSE and MSE are similar at low SNR, but the MLE performs better at high SNR. Finally, results from bit-error-rate simulations reveal that the difference between systems applying the LSE or MLE of CPE is very small for the regarded test case, since the difference in performance only occurs at very high (not practical) SNR values. It can thus be concluded that for 802.11a based MIMO systems, the LSE is well applicable for CPE correction.

Appendix I
Calculation of Gradient and Hessian

The cost function as function of $\boldsymbol{\vartheta}$ is found by substituting $\mathbf{g_0}$ in (9) by $\cos(\boldsymbol{\vartheta}) + j\sin(\boldsymbol{\vartheta})$, resulting in

$$\boldsymbol{\Phi}(\boldsymbol{\vartheta}) = \det(E) \quad , \tag{12}$$

where

$$E = A + \sum_{m=1}^{M} B_m \cos(\vartheta_m) + \sum_{m=1}^{M} C_m \sin(\vartheta_m) \quad , \tag{13}$$

$$\begin{cases} A = \sum_{m=1}^{M} \sum_{p\in\mathcal{P}} \left[\mathbf{x}_m(p)\mathbf{x}_m^H(p) + \mathbf{y}_m(p)\mathbf{y}_m^H(p)\right] \\ B_m = -\sum_{p\in\mathcal{P}} \left[\mathbf{x}_m(p)\mathbf{y}_m^H(p) + \mathbf{y}_m(p)\mathbf{x}_m^H(p)\right] \\ C_m = j\sum_{p\in\mathcal{P}} \left[\mathbf{x}_m(p)\mathbf{y}_m^H(p) - \mathbf{y}_m(p)\mathbf{x}_m^H(p)\right] \end{cases} \tag{14}$$

and $\mathbf{y}_m(p) = \mathbf{H}(p)\mathbf{s}_m(p)$.

From (12) the mth element of the gradient vector $\mathbf{d} = \partial\boldsymbol{\Phi}(\boldsymbol{\vartheta})/\partial\boldsymbol{\vartheta}$ is found to be

$$d_m = \sum_{k=1}^{N_r} \det\left(\breve{E}_k\right) \quad , \tag{15}$$

where $\breve{E}_k$ is identical to E, as defined above, but the kth row is replaced by the kth row of $-B_m \sin(\vartheta_m) + C_m \cos(\vartheta_m)$.

From (12) the (q, r)th entry of the Hessian matrix is found to be

$$G_{q,r} = \frac{\partial^2 \boldsymbol{\Phi}(\boldsymbol{\vartheta})}{\partial\vartheta_q \partial\vartheta_r} = \begin{cases} \sum_{k=1}^{N_r}\sum_{l=1}^{N_r} \det\left(\breve{E}_{k,l}\right) \quad , & \text{if } q = r \\ \sum_{k=1}^{N_r}\sum_{l=1}^{N_r} \det\left(\tilde{E}_{k,l}\right) \quad , & \text{if } q \neq r \end{cases} \tag{16}$$

where $\breve{E}_{k,l}$ is identical to $\breve{E}_k$, except that the lth row is replaced by the lth row of

$$\begin{cases} -B_m \sin(\vartheta_m) + C_m \cos(\vartheta_m) \quad , & \text{if } l \neq k \\ -B_m \cos(\vartheta_m) - C_m \sin(\vartheta_m) \quad , & \text{if } l = k \end{cases} \tag{17}$$

$\tilde{E}_{k,l}$ is also identical to $\breve{E}_k$, except that the lth row is replaced by the lth row of

$$\begin{cases} -B_m \sin(\vartheta_m) + C_m \cos(\vartheta_m) \quad , & \text{if } l \neq k \\ 0 \quad , & \text{if } l = k \end{cases} \tag{18}$$

References

[1] T. Pollet, M. van Bladel, and M. Moeneclaey, "Ber sensitivity of ofdm systems to carrier frequency offset and wiener phase noise," *IEEE Trans. on Commun.*, vol. 43, no. 2/3/4, pp. 191–193, Feb./Mar./Apr. 1995.

[2] A.G. Armada and M. Calvo, "Phase noise and subcarrier spacing effects on the performance of an ofdm communication system," *IEEE Commun. Letters*, vol. 2, no. 1, pp. 11–13, Jan. 1998.

[3] P. Robertson and S. Kaiser, "Analysis of the effects of phase-noise in orthogonal frequency division multiplex (ofdm) systems," in *Proc. Int. Commun. Conf. 1995*, 1995, vol. 3, pp. 1652–1657.

[4] K. Nikitopoulos and A. Polydoros, "Compensation schemes for phase noise and residual frequency offset in ofdm systems," in *Proc. IEEE Global Telecommun. Conf. 2001*, 2001, pp. 330–333.

[5] R.A. Casas, S.L. Biracree, and A.E. Youtz, "Time domain phase noise correction for ofdm signals," *IEEE Trans. on Broadcasting*, vol. 48, no. 3, pp. 230–236, Sept. 2002.

[6] Songping Wu and Y. Bar-Ness, "Multiple phase noise correction for ofdm/sdma," in *Proc. IEEE Global Telecommun. Conf. 2003*, 2003, vol. 3, pp. 1311 – 1315.

[7] T.C.W. Schenk and P. Mattheijssen, "Analysis of the influence of phase noise in mimo ofdm based wlan systems," in *Proc. Symp. IEEE Benelux Chapt. on Commun. and Veh. Techn. (SCVT2003)*, Nov. 2003, pp. 1–8.

[8] Y. Bard, *Nonlinear Parameter Estimation*, Academic Press, NY, 1974.

[9] Xiao-Jiao Tao, Cai-Rong Cao, and Zhen-Ya He, "Passive target tracking using maximum likelihood estimation," *IEEE Trans. on Aerospace and Electronic Systems*, vol. 32, no. 4, pp. 1348–1354, Oct. 1996.

[10] *IEEE 802.11a standard*, ISO/IEC 8802-11:1999/Amd 1:2000(E).

[11] A. van Zelst and J.S. Hammerschmidt, "A single coefficient spatial correlation model for multiple-input multiple-output (mimo) radio channels," in *Proc. URSI XXVIIth General Assembly*, Aug. 2002, pp. 1–4.